JOURNAL OF THERMOPHYSICS AND HEAT TRANSFER
Vol. 10, No. 1, January–March 1996

Mesh Generation and Numerical Simulation of Fluid Entering a Large Tube Bundle

Darrell W. Pepper*
University of Nevada, Las Vegas, Las Vegas, Nevada 89154-4027
and
Barry R. Dyne†
Tanner Research, Inc., Pasadena, California 91107

A three-dimensional finite element model is used to calculate fluid entering a tank containing a large array of tubes (assemblies). The time-dependent primitive equations of fluid motion are solved using equal order, isoparametric hexahedral elements. Petrov–Galerkin weighting, mass lumping, and reduced integration are utilized with explicit time marching. The tank is 7.5 m tall by 6.7 m in diameter, and contains a total of 600 tubes, consisting primarily of 10.8-cm-diam assemblies with some 2.5-cm-diam control rods. The 10.8-cm assemblies are hollow and thin shelled; the 2.5-cm control rods are solid. The fluid first flows into a plenum, then begins to drain into the assemblies, which are positioned below the plenum; the fluid subsequently discharges from the ends of the assemblies near the bottom of the tank and recirculates within the tank prior to returning to the plenum. A total of 623,040 elements was used to discretize the plenum and tank vessel. Over 30 MW of storage were required to execute the problem on a Cray Y-MP, necessitating the use of a special Cray sparse matrix solver. The numerical results predict a marked decrease in the amount of fluid available to the interior tubes.

Nomenclature

$A(V)$ = advection matrix
C = gradient operator
F = load vector
K = diffusion matrix
K_v = K/R_e
L = length
M = mass matrix
N = shape function
n = unit vector normal to surface
p = pressure
Re = Reynolds number
t = time
u = horizontal velocity component, x
V = velocity vector
v = lateral velocity component, y
W = weight, $\equiv N$
w = vertical velocity component, z
x = horizontal direction
y = lateral direction
z = vertical direction
β = Petrov–Galerkin weighting
Γ = boundary
γ = Petrov–Galerkin parameter
ν = kinematic viscosity
ρ = density
Ω = problem domain
∇ = gradient operator, ∇^2 is the Laplacian operator

Subscripts
i, j, k = local node numbering, also denotes column and row vectors
∞ = reference

Superscripts
T = transpose
x = x direction
y = y direction
z = z direction
$*$ = dimensional quantity

I. Introduction

THE study of convective flow in tube bundles has been conducted for many years, much of which is associated with heat exchanger design and nuclear reactor safety. Symolon et al.[1] conducted experiments and model simulations using Cobra-wc,[2] which is a computer code for single-phase multiassembly thermal hydraulic transient analysis, to describe mixed convection flow in a 4 × 4 vertical rod bundle. They succeeded in establishing criteria for the onset of recirculation and established flow regime maps for forced and mixed convection. A simple two-channel model of the rod bundle was formulated. Similar studies performed by Bates and Kahn[3] examined a water-cooled 2 × 6 rod bundle with the lower half of the rod bundle heated. Chawla and Ishii[4] studied the fundamental relations for thermal hydraulic analysis in pin bundles; they discussed two-phase flows with turbulence based on the unsteady, compressible equations of motion, which were area averaged (over a channel). In these model simulations, flow was assumed to be axially dominant, analogous to boundary-layer flows. A number of numerical simulations were also carried out by Rowe[5,6] for transient subchannel analyses of flow within nuclear rod bundles.

More recently, Fagley[7] used the Phoenics code[8] to solve the steady-state, axisymmetric equations for laminar flow, heat transfer, and species transport (five species) within tubular reactors associated with ethane pyrolysis. The finite volume simulation permitted solutions for velocities, temperatures, and concentrations for Reynolds numbers of 1 ×

Presented as Paper 93-2794 at the AIAA 28th Thermophysics Conference, Orlando, FL, July 6–9, 1993; received Aug. 12, 1993; revision received April 14, 1994; accepted for publication July 20, 1995.

*Associate Professor, Department of Mechanical Engineering. Associate Fellow AIAA.
†Special Projects Engineer, 180 N. Vinedo Ave. Member AIAA.

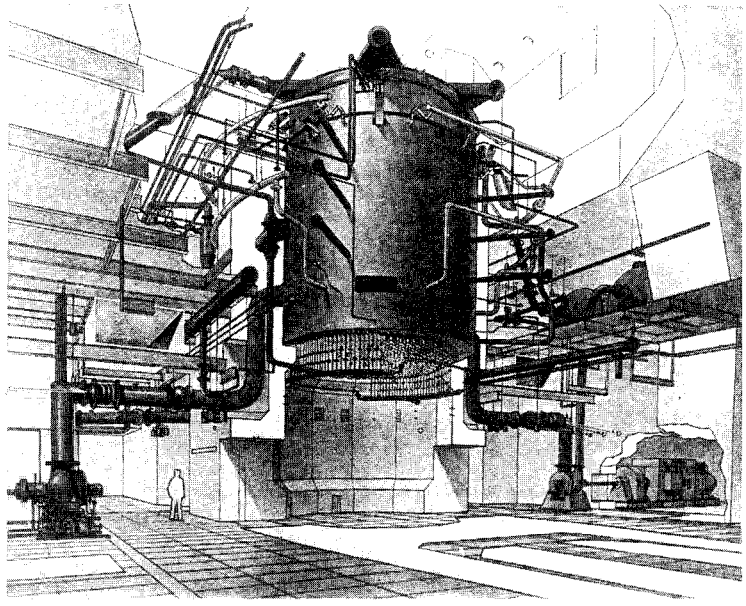

a)

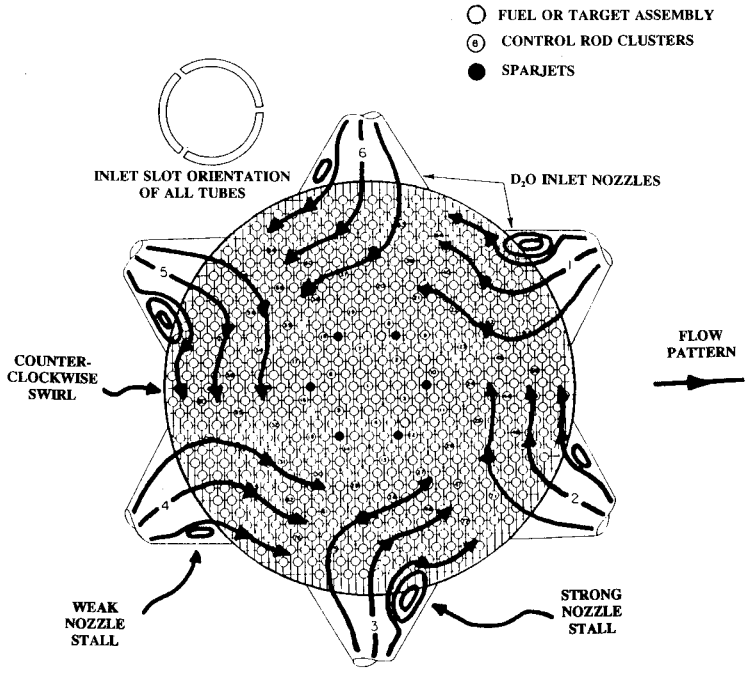

b)

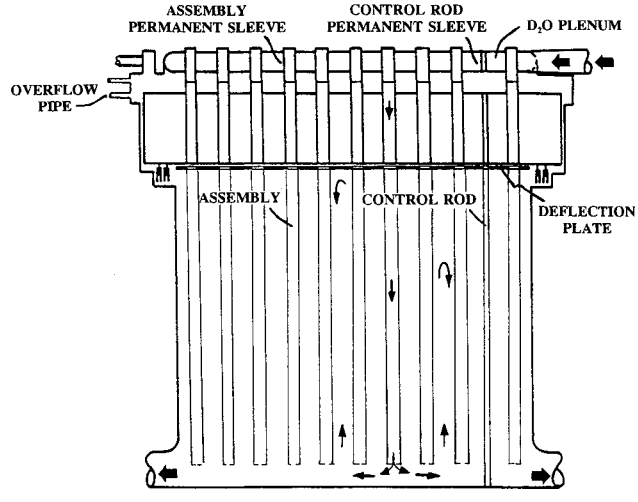

c)

Fig. 1 Plenum and reactor tank geometry: a) reactor complex, b) plenum, and c) tank.

10^2–4×10^2. Wung and Chen[9] used a finite analytic method to calculate convective crossflows in both in-line and staggered tube arrays. The geometries were handled using boundary-fitted coordinates and the stream function vorticity and energy equations solved for Reynolds numbers of 4×10^1, 1.2×10^2, 4×10^2, and 8×10^2. The majority of studies deal with experimental and/or computational flow simulations within small bundle arrays; few have examined flows for tube arrays with large ARs.[10–12] Experimental and numerical studies involving flows into large arrays of tubes with high ARs are essentially nonexistent in the open literature.

In this study, the flow of water entering a large array of tubes (assemblies) is simulated using the incompressible viscous form of the Navier–Stokes equations. Because of the irregular pattern of the tubes an unstructured mesh is generated to discretize the problem domain and a modified finite element method (FEM) is used to solve the governing equations. The problem definition and geometry stem from previous work undertaken to examine heavy water coolant flow within the K-reactor located at the Savannah River Site in Aiken, South Carolina.[13] The K-reactor is one of five unique reactors built in the 1950s to produce weapons-grade nuclear material. In the K-reactor, coolant (or moderator) flows into a large plenum that sits above the assemblies; the moderator drains from the plenum into a large array of 10.8-cm-diam tubes (source and target assemblies) that reside within the tank vessel (refer to Figs. 1a–1c). (Note that the majority of commercial light water reactors are designed with vessel components whose flow patterns are essentially one-dimensional in character and typically flow upward.) Simple one-dimensional hydraulic models, or approximated multi-dimensional models have been examined for such flows (e.g., Cobra,[14] Trac,[15] Relap5[16]); unfortunately, such simplifications are not practical in simulating flow patterns within the K-reactor.

A detailed hydraulic model of the K-reactor has never been developed to fully ascertain flow patterns during normal operations, as well as possible accident situations. The reactors at Savannah River were initially designed to operate at 350-MW thermal power; over the years, the reactors were upgraded to increase material output, reaching nearly 3000 MW. The flow patterns within the K-reactor are known to exhibit nozzle stalls and swirl patterns[17] (see Fig. 1b). Such complex flow patterns cannot be realistically simulated using empiricism and potential flow theory. In addition, a need has existed for some time for a three-dimensional reactor tank vessel transport model to track gadolinium nitrate solution (a neutron poison injection) throughout the moderator space for various types of accident scenarios. Gadolinium nitrate enters the reactor vessel through special tubes (sparjets) located within the reactor and discharges into the surrounding moderator space. The sparjets contain special orifices for injecting the solution, in the form of jets, into the heavy water moderator at regular vertical spacings.

Based on historical bulk moderator temperature measurements during normal operation, flow patterns within the K-reactor vessel consist of multiple regions of recirculating cells.[17] Variable mean flow directions out the discharge pipes located near the bottom of the vessel also occur. Coarse measurements of flow patterns within a nonprototype unheated moderator space were made in a mock-up crossflow tank.[17] Such flows cannot be directly measured while the reactor is operating. Consequently, the flow patterns are only suspected, and not confirmed.

II. Problem Geometry and Mesh

Top and cross-sectional views of the plenum and reactor tank vessel with the assemblies are shown in Figs. 1b and 1c; the entire coolant system is closed. Moderator fluid enters the plenum through the six nozzles as shown in Fig. 1b. As the plenum fills, moderator begins to drain into the assemblies positioned below the plenum. The fluid exits the assembly interiors near the bottom of the reactor tank and recirculates among the assemblies. The moderator eventually exits the tank by way of six discharge pipes at the base of the tank; these discharge pipes are connected to large heat exchangers that cool the moderator before returning it to the plenum to repeat the cycle. Slits (0.63 cm wide) in the assembly housings (i.e., permanent sleeves) within the plenum allow the moderator to flow downward into the assemblies. A total of 600 assemblies are housed within the reactor vessel. These tubes consist of 10.8-cm-diam fuel (source) and target assemblies, and 2.5-cm-diam control rods, which become heated during reactor operations (>100°C).

The generation of a suitable computational mesh remains one of the most nettlesome problems associated with the numerical solution of the partial differential equations (PDEs) of fluid flow. This is especially true for three-dimensional configurations; the effort required to generate an acceptable mesh increases rapidly with increasing geometric complexity

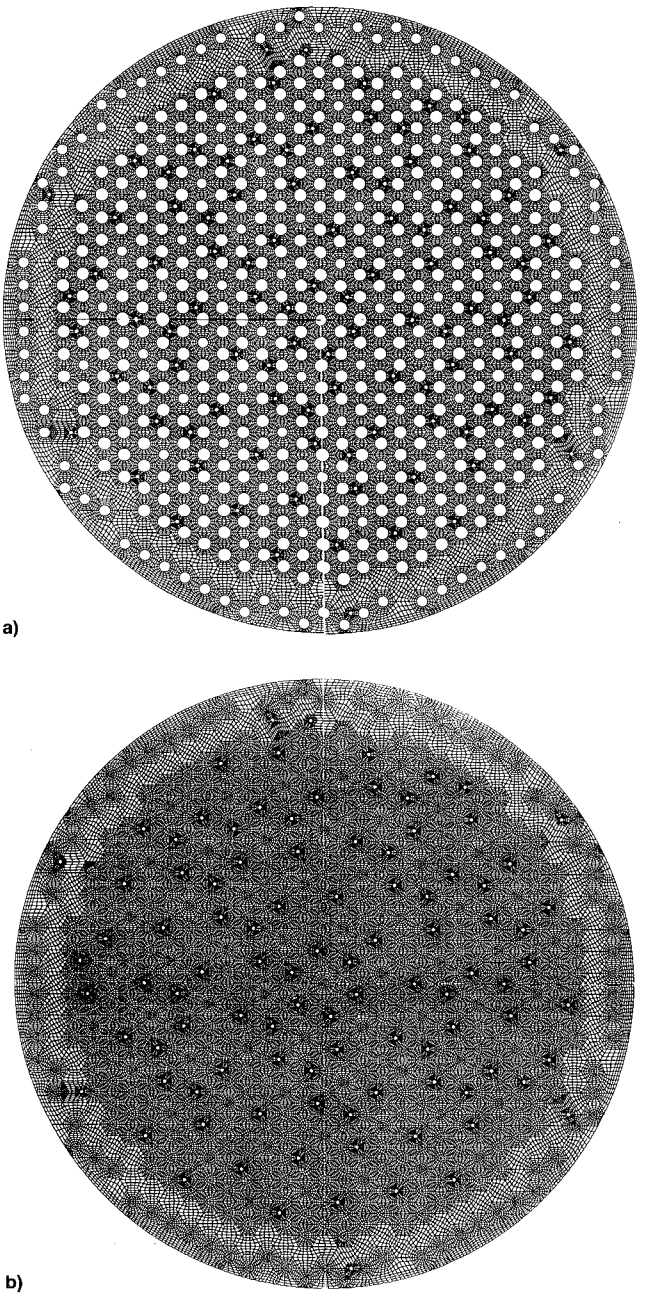

Fig. 2 Computational mesh of reactor tank (two-dimensional slice): a) midplane and b) bottom.

(and likewise quickly becomes prohibitive). In this study, the commonly used practice of grid patching for unstructured grids was employed. The grid patching technique employs disjoint subdomains (or macroregions discretized using macroelements), which share common boundaries among regions. Patran,[18] a commercial grid generation package that utilizes grid patching, was employed to develop the set of grids.

The problem geometry was discretized into two parts: 1) the plenum and 2) the reactor tank. The plenum geometry and nozzles were discretized first; once this element mesh was established, the mesh for the reactor tank was generated and matched to the plenum (i.e., assemblies). Both element meshes were checked to ensure proper boundary conditions: 1) no flow surfaces along all walls and tube surfaces, 2) uniform inflow from the nozzles into the plenum, 3) outflow (drainage) from assembly ports in the plenum into the assemblies in the tank, and 4) outflow from the tank discharge pipes (ultimately returning the fluid to the plenum through the nozzles). Mass conservation was checked for inflow into the assemblies within the plenum and discharge into the tank (from the ends of the assemblies near the bottom of the tank). Note that detailed flow calculations down the 10.8-cm assemblies were not calculated, nor the return flow out the discharge pipes.

Figures 2a and 2b show the generated mesh configurations for a cross-sectional cut through the midplane and near the bottom of the reactor tank. The total number of nodes required for a full discretization of the plenum was 225,101, the number of elements was 202,920. A typical mesh construction for the 10.8- and 2.5-cm housings (which contain the assemblies), within the plenum is shown in Fig. 3. The smaller 2.5-cm rod positions required considerably more nesting of the elements in order to simulate the flow as it passed around the rods. A three-dimensional perspective view of the mesh is shown in Fig. 4. The total number of nodes for the reactor tank vessel was 517,538, the number of elements was 420,120. A horizontal slice through the midplane of the tank shows 47,695 nodes and 41,751 elements; the bottom of the tank required 57,842 nodes and 56,538 elements. This difference is due to the asymmetry of the tank near the bottom, and the presence of end-fittings attached to the ends of the assemblies (to monitor flow); Pepper and Watterberg[19] discuss modeling of the flow within the end-fittings. A total of nine three-dimensional element levels was constructed for the tank, with a higher concentration of elements near the top and bottom of the tank. The size of the assemblies and control rods within the plenum is larger than in the reactor; this is because the plenum consists of housings (i.e., sleeves) in which the assemblies and control rods are inserted and removed from the reactor.

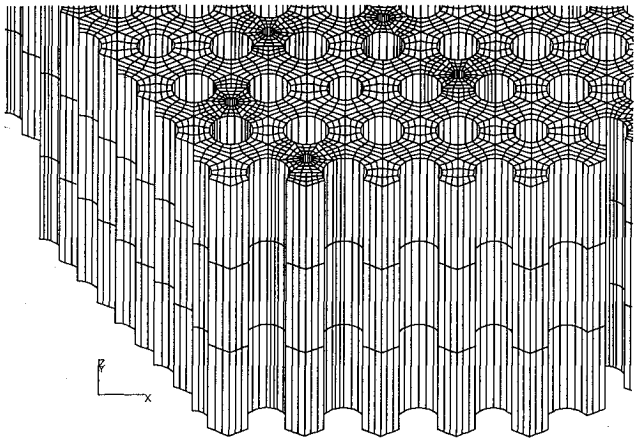

Fig. 3 Three-dimensional perspective view of tank mesh.

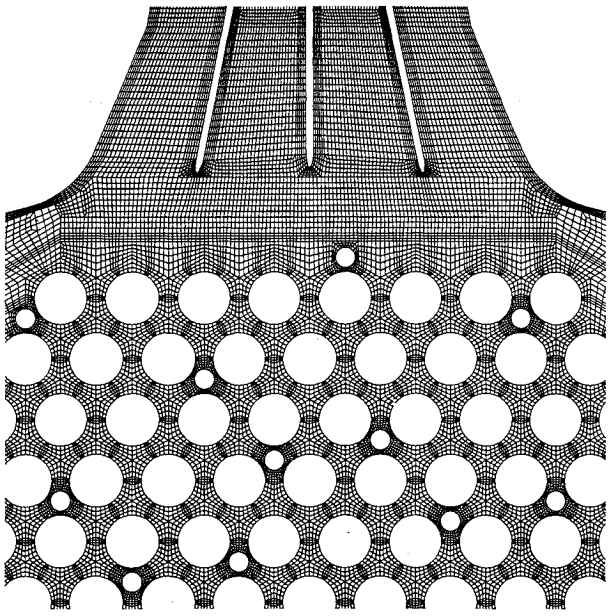

Fig. 4 Mesh pattern within plenum.

III. Mathematical Formulation

The governing equations for conservation of mass and momentum are

$$\nabla \cdot \boldsymbol{V}^* = 0 \tag{1}$$

$$\frac{\partial \boldsymbol{V}^*}{\partial t^*} + (\boldsymbol{V}^* \cdot \nabla)\boldsymbol{V}^* = -\frac{1}{\rho_\infty^*} \nabla p^* + \nu \nabla^2 \boldsymbol{V}^* \tag{2}$$

We define the following nondimensional variables:

$$\begin{gathered} t = t^* \alpha / L^2, \qquad x = x^*/L, \qquad \nabla = \nabla^* L \\ \boldsymbol{V} = \boldsymbol{V}^*/V_\infty, \qquad p = p^*/(\rho_\infty^* V_\infty^2) \end{gathered} \tag{3}$$

where L is the tank height. The dimensional form of the governing equations can be rewritten in nondimensional form as

$$\nabla \cdot \boldsymbol{V} = 0 \tag{4}$$

$$\frac{\partial \boldsymbol{V}}{\partial t} + (\boldsymbol{V} \cdot \nabla)\boldsymbol{V} = -\nabla p + \frac{1}{Re} \nabla^2 \boldsymbol{V} \tag{5}$$

where $Re = V^* L/\nu$. No-slip boundary conditions are assumed for the velocities on the plenum and tank walls as well as the external surfaces of the assemblies and rods. A uniform inflow is assumed at the plenum nozzles.

IV. FEM

The standard weak formulation of the Galerkin weighted residual technique is employed to cast the conservation equations into their integral form:

$$\int_\Omega W(\nabla \cdot \boldsymbol{V})\, d\Omega = 0 \tag{6}$$

$$\int_\Omega \left\{ W \left[\frac{\partial \boldsymbol{V}}{\partial t} + (\boldsymbol{V} \cdot \nabla)\boldsymbol{V} + \nabla p \right] + \frac{1}{Re} \nabla W \cdot \nabla \boldsymbol{V} \right\} d\Omega - \int_\Gamma \frac{1}{Re} W \boldsymbol{n} \cdot (\nabla \boldsymbol{V})\, d\Gamma = 0 \tag{7}$$

The boundary integrals, which arise out of application of Green's identity on the viscous terms, provide a natural mechanism for implementing flux boundary conditions.

Trilinear, eight-noded, isoparametric hexahedral elements are used to discretize the problem domain. The nondimensional velocity vector and pressure are replaced by the trial approximations

$$V(x, y, z, t) = \sum_{i=1}^{n} N_i(x, y, z)V_i(t) \tag{8}$$

$$p(x, y, z, t) = \sum_{i=1}^{n} N_i(x, y, z)p_i(t) \tag{9}$$

where N_i is the trilinear basis function and n is the number of local nodes per element.

Equations (7) and (8) can be written in matrix equivalent forms by setting W equal to N_i. Note that the weighting function in the advection matrix is not set equal to N_i, but rather to a Petrov–Galerkin weighting scheme, which will be discussed later. The resulting matrix equations for mass conservation and velocity are

$$C^T\{V\} = 0 \tag{10}$$

$$[M]\{\dot{V}\} + [K_V]\{V\} + [A(V)]\{V\} + C\{p\} = \{F_V\} \tag{11}$$

where [ ] denotes an $n \times n$ sparse matrix, { } is the column vector of n unknowns, and the $\cdot$ refers to time differentiation of the nodal quantities. The matrix coefficients are defined (using Green's identity for the viscous terms) as

$$[M] = \int_\Omega N_i N_j \, d\Omega \tag{12}$$

$$[K] = \int_\Omega \left(\frac{\partial N_i}{\partial x}\frac{\partial N_j}{\partial x} + \frac{\partial N_i}{\partial y}\frac{\partial N_j}{\partial y} + \frac{\partial N_i}{\partial z}\frac{\partial N_j}{\partial z} \right) d\Omega \tag{13}$$

$$[A(V)] = \int_\Omega N_i \left(u_k N_k \frac{\partial N_j}{\partial x} + v_k N_k \frac{\partial N_j}{\partial y} + w_k N_k \frac{\partial N_j}{\partial z} \right) d\Omega \tag{14}$$

$$C: \quad C^x = \int_\Omega N_i \frac{\partial N_j}{\partial x} \, d\Omega, \qquad C^y = \int_\Omega N_i \frac{\partial N_j}{\partial y} \, d\Omega$$
$$C^z = \int_\Omega N_i \frac{\partial N_j}{\partial z} \, d\Omega \tag{15}$$

$$C^T = \begin{Bmatrix} C^x \\ C^y \\ C^z \end{Bmatrix} \tag{16}$$

$$\{F_V\} = \frac{1}{Re} \int_\Gamma N_i(n \cdot \nabla V) \, d\Gamma \tag{17}$$

where the i, j, k subscripts denote summation over the local nodes within an element (e.g., N_i or N_k would be a column vector eight nodes long while N_j would be a single eight-node row vector), $[K_V] = [K]/Re$, and $d\Gamma$ represents the boundary elements where fluxes are specified. The C terms expressed by Eq. (15) are gradient operators.[20] Normally $2 \times 2 \times 2$ Gaussian quadrature is used in the numerical evaluation of these equations. However, in regions where elements are uniform, reduced integration (one point quadrature) is used to enhance solution speed.[20]

A. Petrov–Galerkin Weighting

To stabilize the discretized advection terms, an anisotropic balancing diffusion is introduced into each governing equation using a Petrov–Galerkin weighting function.[21] This function is obtained by perturbing the weight such that

$$W_i = N_i + \gamma(h_e/2|V|)(V \cdot \nabla N_i) \tag{18}$$

$$h_\xi = (x_{2\xi} - x_{1\xi})\hat{i} + (y_{2\xi} - y_{1\xi})\hat{j} + (z_{2\xi} - z_{1\xi})\hat{k}$$
$$h_\eta = (x_{2\eta} - x_{1\eta})\hat{i} + (y_{2\eta} - y_{1\eta})\hat{j} + (z_{2\eta} - z_{1\eta})\hat{k}$$
$$h_\zeta = (x_{2\zeta} - x_{1\zeta})\hat{i} + (y_{2\zeta} - y_{1\zeta})\hat{j} + (z_{2\zeta} - z_{1\zeta})\hat{k}$$
$$h_e = \frac{1}{|V|}(|V \cdot h_\xi| + |V \cdot h_\eta| + |V \cdot h_\zeta|)$$

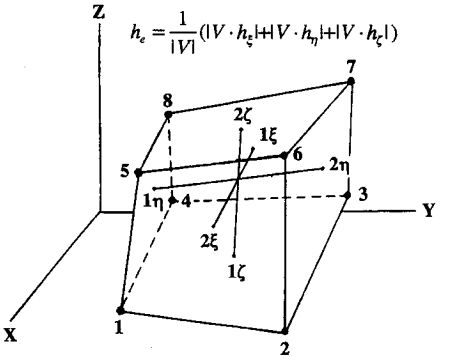

Fig. 5 Hexahedral element with mesh length vectors.

where h_e is the element mesh length and $|V|$ denotes the magnitude of the velocity vector. The calculation of h_e utilizes the element geometry and the three mesh length vectors shown in Fig. 5. For the mesh length along V, these vectors, which intersect the element at the midpoints of the sides, are projected in the direction of the local velocity to obtain

$$h_e = (1/|V|)(|h_\xi \cdot V| + |h_\eta \cdot V| + |h_\zeta \cdot V|) \tag{19}$$

The parameter γ is defined as

$$\gamma = \coth(\beta/2) - (2/\beta) \tag{20}$$

where $\beta = |V|h_e R_e/2$ is used for the momentum equations. This form of anisotropic balancing diffusion acts in the direction of the propagation of the perturbation (velocity field). The precise amount of artificial diffusion (for eliminating the shortest waves) and direction in which it must be added for optimizing accuracy are calculated for each element.

B. Temporal Integration

Mass lumping is employed to permit explicit time integration without the need for total matrix inversion. In this instance, the consistent mass matrix row values are summed into single diagonal values; the inverse of the mass matrix becomes $[M]^{-1} = 1/[M_l] \equiv [M_l]^{-1}$. The lumped mass matrix is formed directly in the assembly process by the approximation

$$[M_l] = \int_\Omega N_i \left(\sum_{j=1}^{n} N_j \right) d\Omega \tag{21}$$

thus eliminating the need for the consistent mass matrix formulation given by Eq. (12).

The velocity is solved using an explicit Euler scheme

$$\{V\}^{n+1} = \{V\}^n + \Delta t[M_l]^{-1}(\{F_V\} - [K_V]\{V\}^n - [A(V)]\{V\}^n - C\{p\}^n) \tag{22}$$

where the superscript n indicates quantities evaluated at time $n\Delta t$, with Δt being the time step. To maintain stability both the Courant and diffusive limits associated with an explicit forward Euler scheme are calculated over each element and the time step is adjusted to permit global stability.

C. Pressure Poisson Equation Solution

Unlike the velocity, which may be marched explicitly in time, the pressure in an incompressible flow requires the solution of a Poisson equation. The solution of a Poisson equa-

tion on the reactor tank grid posed a significant challenge due to the large number of equations involved. A major portion of the code development effort was spent toward finding a computationally feasible solution method.

The pressure equation is usually obtained by taking the derivative of each of the momentum equations with respect to their principal directions and combining the three equations. The resulting equation becomes a Poisson equation for pressure with the right-hand side (RHS) consisting of terms containing gradients of the velocity components. We can construct this equation numerically by taking the derivatives of the discretized momentum equations [using Eq. (15)] and combining the second derivative pressure terms.[22] Applying the method of weighted residuals, we obtain the following discretized Poisson equation:

$$[K]\{p\} = C^T[M_l]^{-1}(\{F_v\} - [K_v]\{V\} - [A(V)]\{V\}) \quad (23)$$

where $\{F_v\}$ contains the body force terms and boundary conditions associated with the momentum equations, and $[K]$ is the sparse symmetric matrix for the Laplacian operator (∇^2) [Eq. (13)]. Since the converged solution of Eq. (23) can be an expensive procedure, overall performance can be improved by subcycling the pressure solution.[22] Velocities are calculated over several time steps between solutions of Eq. (23); during these interim transient calculations, the pressure is updated using the simple extrapolation relation

$$\{p\}^{n+1} = 2\{p\}^n - \{p\}^{n-1} \quad (24)$$

D. Storage

One of the most commonly used matrix solution methods in finite element algorithms is skyline storage coupled with a direct solution method, e.g., Cholesky decomposition followed by back substitution. The skyline technique stores the matrix column by column, in a one-dimensional array, retaining only the values between the uppermost nonzero value of a column and the diagonal. Following this strategy, it was determined that 15 billion words (BW) of storage would be required to store and solve the pressure matrix equation in the one-dimensional skyline format, plus some additional storage for pointer arrays. This was obviously an unacceptable requirement and other strategies were investigated.

Because direct methods complete the solution in a fixed number of operations, whereas iterative methods rely on a convergence test for completion, it was initially decided to pursue a direct solution strategy and to try to reduce the storage requirements. This is typically accomplished by using various mesh optimization algorithms that renumber the nodes of the mesh to reduce the bandwidth or skyline of the associated matrix. The most common of these techniques are the Gibbs–Poole–Stockmeyer (GPS), Gibbs–King (GK), Cuthill–McKee (CM), and reverse Cuthill–McKee (RCM). Other methods are the profile front minimization (PFM) of Hoit and Wilson[23] and a spectral method being developed by Simon.[24] These methods usually require very large amounts of core memory in order to determine the most efficient numbering. In general, there is a tradeoff between storage and CPU time. The PFM method is highly efficient in terms of memory and was implemented based on code listing provided in Hoit and Wilson.[23] While it was shown to be effective on several test cases, it was highly CPU intensive. Efforts to renumber the reactor grid using this algorithm yielded estimates of computation times on the order of months and it was decided that this method was not a feasible approach.

Although simple iterative methods can require more CPU time than direct methods, a good initial guess will always be available, which is the solution from the previous time step. A primary advantage of iterative methods is that they may easily be written to take advantage of the sparsity of the matrix and may provide significant storage savings over direct methods. The matrix corresponding to the reactor grid has a fill of 0.006% (i.e., 0.006% of the coefficients would be nonzero in a classical elimination process) and is thus a prime candidate for sparse iterative solvers. In addition, the properties of positive definiteness and diagonal dominance, required for convergence, are possessed by the matrix. After investigation of both approaches, it was decided to pursue iterative methods.

Several libraries were investigated for solvers of systems of linear equations, for both direct and iterative solvers. The Scilib (Cray Scientific Library) routine Sitrsol[25] was found to be the best for this application. The matrix is stored in an efficient sparse matrix format and several conjugate gradient type solvers are available as options. The Imsl, Nag, and Lapack routines store the matrix in full $n \times n$ format, without taking advantage of the sparsity of the matrix. The Scilib routines are also optimized for Cray machines.

The limited availability of computer resources, especially core memory, were the overriding factor in the selection of solution methodology, and significant effort was expended in developing a version of the code that would run in approximately 30 MW. Minimum storage requirements for the code are shown in Table 1, as well as additional requirements for various options (including temperature).

Because of the explicit nature of the algorithm for the transient equations, the model is suited to parallel computation. A compressible flow version of the model has been run on a MasPar MP-1216 minisupercomputer.[26] The MP-1216 is a massively parallel machine with 16,384 processing elements (nodes), each with its own dedicated data memory. Instead of iterating through a series of DO loops common to three-dimensional computational fluid dynamics (CFD), the MP-1216 assigns one processor element to each data element and carries out the instructions concurrently for all data points. Fortran 90 is used on the MP family of computers.

Table 1 Storage requirements

Usage	Array[a]	Storage, MW
Geometric data		
Coordinates	X, Y, Z	1.41
Connectivity	NODE	3.12
Lumped mass	P	0.47
Velocity BC	NTSU	0.17
Temperature BC	NTST, NTID	0.48
Explicit equations		
RHS	B1-B7	3.29
Solution	U, V, W, T, P	2.35
Poisson equations		
Column pointer	COLSTR	0.47
Row pointer	ROWIND	5.90
Matrix values	VALUES	5.90
Real workspace	WORK	2.35
Intgr workspace	IWORK	0.47
Second-order time		
Previous RHS	B1N-B4N	1.88
Previous sol'n	OU, OV, OW, OT	1.88
Subcycling		
Previous press	OP	0.47
TOTAL		30.61

[a]Letters denote variable names for velocity components, temperature, pressure, and load vectors (i.e., RHS of equations, etc.).

V. Results

Generation of the mesh for the overall tank assembly was conducted in two steps: the plenum and nozzle inlets were discretized first, then the reactor vessel. The grid generation was performed on an IBM RISC 6000 workstation, which was linked to a Cray Y-MP. Graphical output of the mesh and flow results was directed to a Silicon Graphics IRIS 25/D workstation. Once the plenum mesh was completed and checked, the mesh within the reactor vessel was generated and tested. The generation of the complete mesh for the

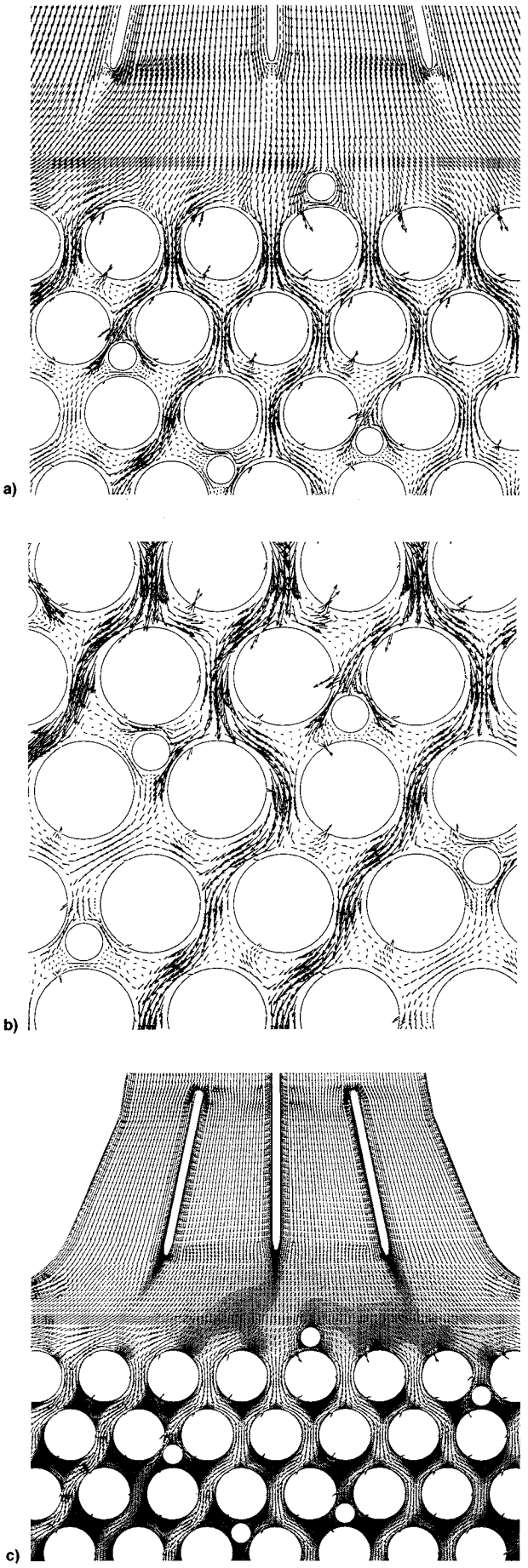

Fig. 6 Velocity vectors within plenum: a) near nozzle, b) close-up of flow into slits, and c) velocity vectors overlaid on pressure contours.

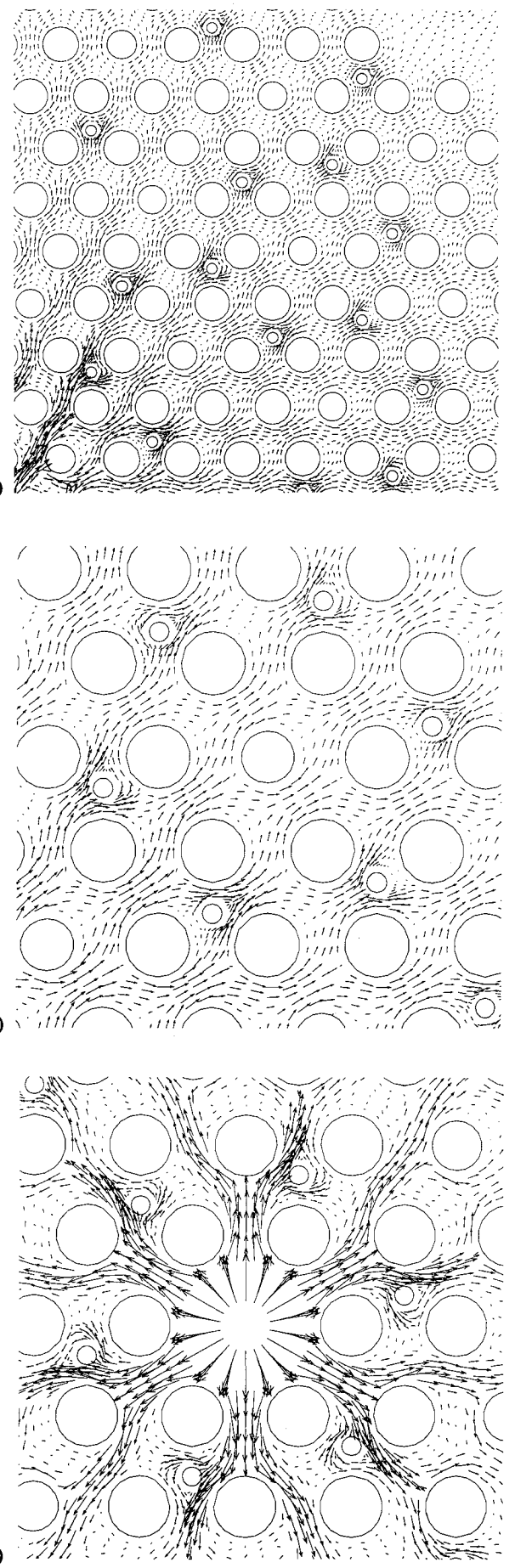

Fig. 7 Velocity vectors within tank: a) tank interior, b) close-up of velocity vectors, and c) flow originating from a single assembly.

reactor complex required several months of testing and verification before a flow solution was attempted.

A. Plenum

Fluid entering from the nozzles into the array of tube housings within the plenum was simulated first. Several remeshings were required before the final mesh configuration was obtained. These remeshings were necessary in order to determine the most optimum configuration for obtaining convergent flow distributions (i.e., the solution would not oscillate or cease to develop after only a few initial time steps).

Figures 6a–6c show a portion of the plenum for one nozzle and the beginning of the tube array within the plenum. In Fig. 6a the coolant flows around the three turning vanes (originally designed to spread the flow distribution) and enters the tube array. As the fluid enters the first few rows of tubes, some of the fluid begins to enter the assemblies through the three slits cut in each tube (Fig. 6b). Numerous crossflow recirculation zones occur within the array. Velocity vectors overlaid onto pressure contours (gray scale) are shown in Fig. 6c. The asymmetry in the flow distribution is due in part to the placement of the control rods within the assembly array (acting to block the flow path). The amount of fluid begins to drop off towards the center of the plenum (mass balance indicated more fluid draining into the outer rows of assemblies than in the center array). This phenomena is not surprising for low inlet flows from the nozzles, and implies serious consequences if a loss of coolant accident (LOCA) were to occur. The flow rate of emergency coolant must be sufficient enough to overcome the rapid drainage effect from the tubes near the nozzles to prevent assembly starvation within the center of the tank (and subsequent failure due to heating).

B. Reactor Tank

To test the accuracy of the reactor tank mesh, source flow from a single assembly was initially simulated near the midplane of the reactor tank. Figures 7a–7c show velocity vector plots around the 2.5- and 10.8-cm positions; the flow accelerates within the spaces among the 2.5- and 10.8-cm assemblies in Fig. 7c. Once the mesh density was established, flows entering all of the assemblies in the plenum were used to establish the flows exiting from the assemblies near the bottom of the tank. Figure 8 shows vertical velocities near the center of the reactor vessel (after discharging from the ends of the assemblies into the reactor tank).

Displays of the mesh (cross section) and resultant velocity vectors near the bottom of the tank are shown in Figs. 9a–

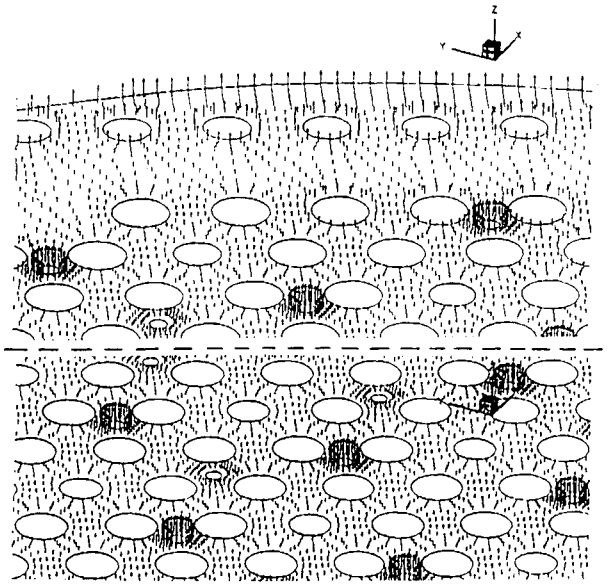

Fig. 8 Three-dimensional flow near midplane of tank.

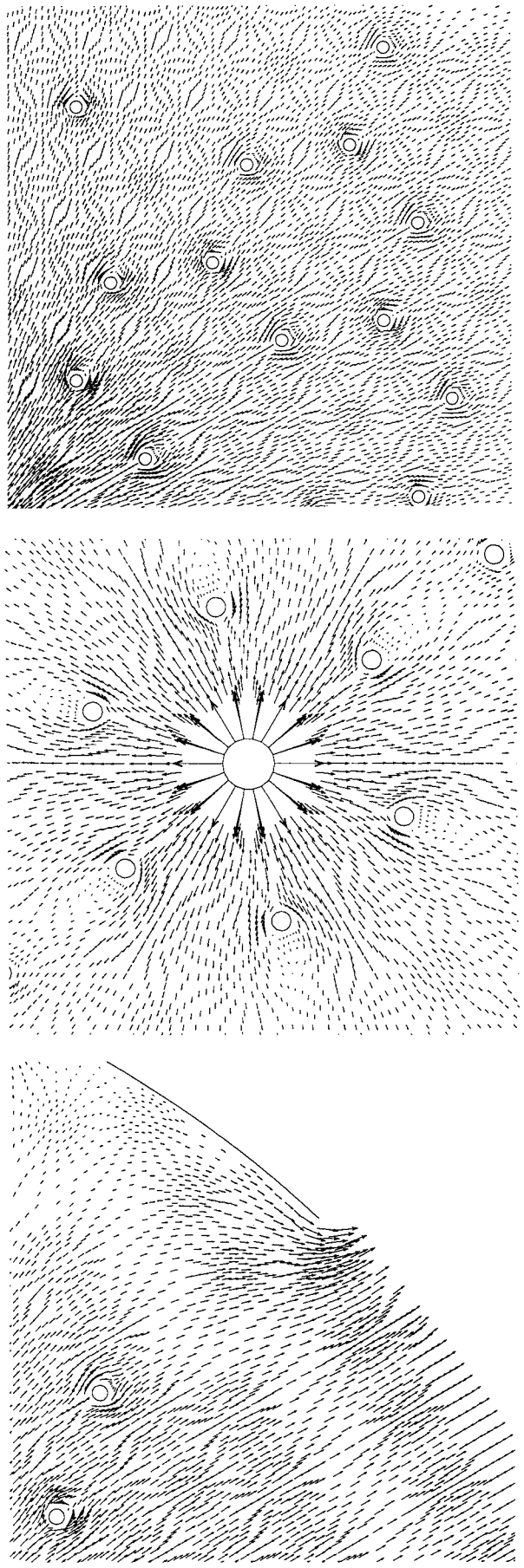

Fig. 9 Velocity vectors near bottom of tank: a) near bottom of tank, b) flow originating from a single assembly, and c) velocity vectors near discharge pipe.

9c. For the levels near the bottom of the tank, the element structure is somewhat different than the midplane elements; this is due to the termination of the assemblies and introduction of end-fittings at the tank bottom.[19] The outflow from the assemblies was matched with the flow boundary conditions generated within the plenum solution. Figure 9b shows velocity vectors emanating from an assembly near the center of the array at the bottom of the reactor tank. The flow accelerates around the 2.5-cm positions; the seemingly unusual pattern of the velocity vectors is due to the orientation of the nodal positions. A close-up view as the flow exits the tank bottom and enters one of the discharge pipes is displayed in Fig. 9c.

It is difficult to obtain a comprehensive picture of the complete flow pattern throughout the reactor: the flow exits from the nozzles and enters the plenum, drains into the assemblies through slits in housings within the plenum, flows down the assemblies, discharges from the assemblies near the bottom of the reactor vessel, and finally recirculates throughout the tank among the assemblies before discharging out the return pipes. This problem geometry is quite complex, and the flow structure equally complex to simulate totally. This is the first effort to completely discretize and attempt a solution throughout the reactor plenum and tank using the full viscous form of the equations of motion for an incompressible fluid. While much has yet to be done, these early results indicate the ability of the three-dimensional finite element algorithm to model such complicated flows within very large arrays in detail. Additional efforts have been undertaken to calculate coolant temperatures associated with free and forced convection within K-reactor (the assemblies are normally heated as a result of neutron bombardment); results from these simulations are still under review. The model should be useful in determining locations where flow starvation can occur, LOCA scenarios, and ultimately predicting regions of high temperatures attributed to decay heat or assembly failure.

VI. Conclusions

A hybrid three-dimensional finite element model and mesh have been developed to calculate incompressible, fluid flow within a large array of tubes enclosed within a cylindrical vessel. The primitive equations of motion are solved using equal order basis functions for the velocities and pressure, Petrov–Galerkin weighting for the advection terms, and mass lumping. The transient equations are solved using an explicit forward Euler scheme. Pressure is obtained using subcycling (extrapolation) with intermittent implicit solution of a Poisson equation.

The large array consists of both 2.5- and 10.8-cm-diam tubes. The 10.8-cm tubes (assemblies) are thin shelled and hollow; slits cut at 120-deg angles in assembly housings within the plenum allow fluid to drain into the assemblies located below within the tank. The 2.5-cm tubes (rods) are assumed solid. This complex configuration of tubes is representative of fuel and target assemblies found within K-reactor, which is a heavy water moderated nuclear production reactor located at the Savannah River Site in Aiken, South Carolina.

The problem geometry was discretized into two parts: 1) plenum and 2) tank vessel. The mesh for the plenum and inlet nozzles required a total of 225,101 nodes (202,920 elements). The reactor tank required 517,538 nodes (420,120 elements). Because of the large number of nodes required for solution of the flows within both the plenum and tank vessel, an iterative scheme especially optimized for performance on a Cray supercomputer was employed for the implicit pressure solution.

The flow results indicate the distribution of fluid within the assembly array is quite complicated, with many regions of separated flow around the tube exteriors. The amount of fluid available to the assemblies decreases towards the center of the array; this is due to the assembly arrangement (and blockage) near the inlet nozzles within the plenum.

Further work is necessary to more closely examine regions of flow separation and starvation of flow to the central assemblies, particularly in the event of a LOCA.

Acknowledgments

We wish to acknowledge the financial support provided by Westinghouse, Savannah River Site under Contract AA89048S. We also wish to thank Larry Koffman and Roger Cooper (retired), both of the Westinghouse Savannah River Site, Aiken, South Carolina, for their technical advice and support of this work.

References

[1]Symolon, P. D., Todreas, N. E., and Rohsenow, W. M., "Criteria for the Onset of Flow Recirculation and Onset of Mixed Convection in Vertical Rod Bundles," *Journal of Heat Transfer*, Vol. 109, 1987, pp. 138–145.

[2]George, T. L., "COBRA-WC: A Version of COBRA for Single-Phase Multiassembly Thermal Hydraulic Transient Analysis," Battelle Pacific Northwest Lab., Rept. PNL-3259, Richland, WA, July 1980.

[3]Bates, J., and Kahn, E., "Investigation of Combined Free and Forced Convection in a 2 × 6 Rod Bundle During Controlled Flow Transients," *AIChE Symposium Series on Heat Transfer* (Orlando, FL), Vol. 76, 1980, pp. 215–230.

[4]Chawla, T. C., and Ishii, M., "Equations of Motion for Two-Phase Flow in a Pin Bundle of a Nuclear Reactor," *International Journal of Heat and Mass Transfer*, Vol. 21, 1978, pp. 1057–1068.

[5]Rowe, D. S., "A Mathematical Model for Transient Subchannel Analysis of Rod-Bundle Nuclear Fuel Elements," *Journal of Heat Transfer*, Vol. 95C, 1973, pp. 221–227.

[6]Rowe, D. S., "COBRA-II, A Digital Computer Program for Thermal Hydraulic Subchannel Analysis of Rod Bundle Nuclear Fuel Elements," Battelle Pacific Northwest Lab., Rept. BNWL-1229, Richland, WA, Feb. 1970.

[7]Fagley, J. C., Jr., "Simulation of Transport in Laminar, Tubular Reactors and Application to Ethane Pyrolysis," *Industrial Engineering Chemical Research*, Vol. 31, No. 1, 1992, pp. 58–69.

[8]Rosten, H., and Spalding, D. B., *The Phoenics Beginner's Guide*, Cham Ltd., London, 1987.

[9]Wung, T. S., and Chen, J. C., "Finite Analytic Solution of Convective Heat Transfer for Tube Arrays in Cross Flow Part I: Flow Field Analysis," *ASME Proceedings of the 1988 National Heat Transfer Conference*, HTD-96, Vol. 3, 1988, pp. 347–353.

[10]Le Quere, P., "A Note on Multiple and Unsteady Solutions in Two-Dimensional Convection in a Tall Cavity," *Journal of Heat Transfer*, Vol. 112, 1990, pp. 965–974.

[11]De Vahl Davis, G., "Finite Difference Methods for Natural and Mixed Convection in Enclosures," *8th International Heat Transfer Conference* (San Francisco, CA), Vol. 1, Hemisphere, Washington, DC, 1986, pp. 101–109.

[12]Roux, B., Grondin, J., Bontoux, P., and De Vahl Davis, G., "Reverse Transition from Multicellular to Monocellular Motion in Vertical Fluid Layer," *Physical and Chemical Hydrodynamics*, Vol. 3F, 1980, pp. 292–297.

[13]Pepper, D. W., "Generation of 3-D Grids for the K-Reactor at the Savannah River Site, Aiken, South Carolina," APRI Systems, Inc., Final Rept., Moorpark, CA, 1992.

[14]Wheeler, C. L., Stewart, C. W., Cena, R. J., Rowe, D. S., and Sutey, A. M., "COBRA-IV-I: An Interim Version of COBRA for Thermal-Hydraulic Analysis of Rod Bundle Nuclear Fuel Elements and Cores," Battelle Pacific Northwest Lab., Rept. BNWL-1962, Richland, WA, 1976.

[15]"TRAC-PF1/MOD1: An Advanced Best-Estimate Computer Program for Pressurized Water Reactor Thermal-Hydraulic Analysis," Los Alamos National Lab., NUREG/CR-3858, LA-10157-MS, Los Alamos, NM, July 1986.

[16]Ransom, V. H., Wagner, R. J., Trapp, J. A., Feinauer, L. R., Johnsen, G. W., Kiser, D. M., and Riemke, R. A., "RELAP5/MOD2 Code Manual Volume 1: Code Structure, Systems Models, and Solution Methods," EG&G Idaho, Inc., NUREG/CR-4312, EGG-2396, Idaho Falls, ID, Aug. 1985.

[17]*DPST-83-282*, E. I. Dupont de Nemours, Savannah River Plant,

Aiken, SC, Jan. 28, 1983.

[18]*PATRAN User's Guide*, Release 2.0, PDA Engineering, Santa Ana, CA, 1986.

[19]Pepper, D. W., and Watterberg, P. A., "Modeling of Convective Mixing Downstream of Separately Heated Annuli," American Society of Mechanical Engineers, Paper 86-HT-38, June 1986.

[20]Pepper, D. W., and Singer, A. P., "Calculation of Convective Flow on the Personal Computer Using a Modified Finite-Element Method," *Numerical Heat Transfer, A*, Vol. 17, 1990, pp. 379–400.

[21]Yu, C. C., and Heinrich, J. C., "Petrov-Galerkin Methods for the Time-Dependent Convective Transport Equation," *International Journal for Numerical Methods in Engineering*, Vol. 23, 1986, pp. 883–901.

[22]Gresho, P. M., Chan, S. J., Lee, R. L., and Upson, C. D., "Modified Finite Element Method for Solving the Time-Dependent Incompressible Navier-Stokes Equations, Part 1: Theory," *International Journal for Numerical Methods in Fluids*, Vol. 4, 1984, pp. 557–598.

[23]Hoit, M., and Wilson, E. L., "An Equation Numbering Algorithm based on a Minimum Front Criteria," *Computers and Structures*, Vol. 16, No. 1–4, 1983, pp. 225–239.

[24]Simon, H., private communication, NASA Ames Research Center, Moffett Field, CA, July 1993.

[25]*Volume 3: UNICOS Math and Scientific Library Reference Manual*, Cray Research, Inc., SR-2081 7.0, Mendota Heights, MN, 1992, pp. 306–318.

[26]Brueckner, F. P., and Pepper, D. W., "Parallel Finite Element Algorithm for Three-Dimensional Inviscid and Viscous Flow," *Journal of Thermophysics and Heat Transfer* Vol. 9, No. 2, 1995, pp. 240–246.